Gain-Scheduling Attitude Control for Complex Spacecraft Based on HOSVD

Bingyao Lei
School of Astronautics,
Beihang University,
Beijing 100191, China
e-mail: by_lei@buaa.edu.cn

Peng Shi[1]
School of Astronautics,
Beihang University,
Beijing 100191, China
e-mail: shipeng@buaa.edu.cn

Changxuan Wen
Key Laboratory of Space Utilization,
Technology and Engineering Center for Space Utilization,
Chinese Academy of Sciences,
Beijing 100094, China
e-mail: wenchangxuan@gmail.com

Yushan Zhao
School of Astronautics,
Beihang University,
Beijing 100191, China
e-mail: yszhao@buaa.edu.cn

In this paper, a robust gain-scheduling attitude control scheme for spacecrafts with large rotational appendages is proposed. First, by introducing the higher-order singular value decomposition (HOSVD) method, a polytopic linear parameter varying (LPV) model with a family of weighting coefficients is developed based on the kinetics of a flexible spacecraft. This model eliminates the need of verifying all the gridding points, which is required in conventional controller synthesis process, and reduces the calculation complexity. Second, a generalized plant is derived to guarantee both the system robust stability and the tracking performances. Based on the LPV control theory, a less conservative controller synthesis condition for the polytopic LPV system is deduced. With an online tuning unit, the convex combination of every vertex controller is obtained. For control implementation, the present scheduling parameter is taken as an input for the tuning unit. Numerical results demonstrate the effectiveness and efficiency of the proposed control scheme. [DOI: 10.1115/1.4041752]

1 Introduction

The stabilization and disturbance attenuation have been the critical objectives in controller design for spacecrafts. With the wide use of large flexible appendages and payloads, the analogous problem is further complicated because of the extra introduction of more external disturbances and system uncertainties. Furthermore, as the solar paddle rotates, modal parameters in low-frequency range show obvious variation [1]. These issues cannot be neglected when high control precision and stability are demanded [2]. However, conventional control schemes based on the linear time invariant (LTI) model exert limitations in practical application. Hence, there is a need for developing more precise model and corresponding control methods to guarantee the closed-loop stability as well as to possess required performances.

Several control strategies have been developed to resolve these problems. The main approach of Refs. [3–5] is to describe the system uncertainty brought by the moment of inertia and external disturbances. By introducing the variable structure in the controller, the uncertainty can be regarded as a perturbation, and its influence on the system response is eliminated through the robustness of the proposed methods. Compared with Refs. [3] and [4], an adaptive sliding mode strategy has been developed in Ref. [5], which guarantees the system exponential convergence without a prior knowledge about the upper bound of the uncertainty. Another alternative solution is to design observers estimating the unknown external torques and uncertain moment of inertia [6–8]. Thus, the estimated information can compensate the corresponding terms in the dynamic model.

Among these advanced control theories, the gain scheduling linear parameter varying (LPV) control was developed about 30 years ago [9]. With the introduction of varying Lyapunov function [10], the controller is less conservative, making it possible to describe the system changing in larger parameter intervals. To further decrease the controller conservativeness, the switching control technique is introduced based on multiple parameter-dependent Lyapunov functions [11–14]. Various switching laws are investigated to pursue a more robust stability performance and transient responses. For instance, the smoothness condition [12–14] is added as an amelioration for nonsmooth transient responses [11]. Due to its characteristics in simplifying difficult nonlinear problems with relatively low computational complexity when conducting online control, the LPV control technique has been a widespread scheme for its effectiveness and low cost, especially in autopilots [15–17] and offshore wind turbine control systems [18–20]. With the introduction of bounded real lemma (BRL), the controller synthesis problem can be transformed into a convex optimization problem in a family of linear matrix inequalities (LMIs) [10]. One great challenge in controller synthesis is the infinite number of LMIs to be verified. The most commonly used method is to grid the value set of system varying parameters [10]. Although without the loss of generality, this process can have high computational complexity in the controller synthesis process, especially when there are several scheduling parameters [21].

Hence, it is expected that the original plant can be approximated in a special form to bypass the gridding phase. Through the tensor product model transformation, the N dimensional tensor is simplified into a series of singular values and the corresponding singular matrices, in which the core tensor is extracted by cutting off some small singular values. With this technique, the derived LPV system can be decomposed into convex combination terms with varying parameters as weighting coefficients [22]. Consequently, it is not complicated to design a controller for the obtained polytopic model because of the large decrease in the LMIs number. Inspired by this, we propose a new LPV control strategy based on higher-order singular decomposition (HOSVD). Considering that the system moment of inertia and coupling matrices are functions of the rotational angle of flexible appendages [2], we set the rotational angle as the scheduling parameter. Based on the polytopic LPV model obtained via HOSVD, the controller synthesis condition is derived to guarantee the closed-loop stability and robustness against disturbances, uncertainties and high vibration mode. Compared with other advanced control approaches, this method demands fairly low online computational complexity, which can be more practical for real-time implementation.

[1]Corresponding author.

Contributed by the Dynamic Systems Division of ASME for publication in the Journal of Dynamic Systems, Measurement, and Control. Manuscript received January 11, 2018; final manuscript received October 11, 2018; published online November 22, 2018. Assoc. Editor: Yang Shi.

2 Preliminaries

DEFINITION 1. *Given the tensor* $\mathbf{A} \in R^{I_1 \times I_2 \times \cdots \times I_N}$, *this tensor can be rewritten as the product of [23]*

$$\mathbf{A} = \mathbf{S} \times_1 \mathbf{U}_{(1)} \times_2 \mathbf{U}_{(2)} \times_3 \ldots \times_N \mathbf{U}_{(N)} = \mathbf{S} \bigotimes_{n=1}^{N} \mathbf{U}_{(n)} \tag{1}$$

where $\mathbf{U}_{(n)} = [\boldsymbol{u}_1^{(n)}, \boldsymbol{u}_2^{(n)}, \ldots, \boldsymbol{u}_{I_n}^{(n)}]$ *represents the* $(I_n \times I_n)$ *matrix in which* $n = 1, 2, \ldots, N$. $\boldsymbol{u}_i^{(n)}$ *is the ith n mode singular vector.* $\mathbf{S}$ *represents a* $(I_1 \times I_2 \times \cdots \times I_N)$ *tensor and its subtensors* $\mathbf{S}_{i_n = i}$ *have the following properties:*

(1) *Any two arbitrary subtensors of* $\mathbf{S}$ *are orthogonal*

$$\langle \mathbf{S}_{i_n=\alpha}, \mathbf{S}_{i_n=\beta} \rangle = 0, (\alpha \neq \beta) \tag{2}$$

(2) *All subtensors are ordered in accordance with their Frobenius norms*

$$\|\mathbf{S}_{i_n=1}\| \geq \|\mathbf{S}_{i_n=2}\| \geq \ldots \geq \|\mathbf{S}_{i_n=I_n}\| \geq 0 \tag{3}$$

Remark 1. By applying the above concepts to the LPV system, the original system with time varying parameter that changes in the closed hypercube, $\Omega = [a_1, b_1] \times [a_2, b_2] \times \cdots \times [a_N, b_N]$, can be transformed into a polytopic LPV form. First, the closed hypercube is gridded into I_i in each $[a_i, b_i]$, $i = 1, \ldots, N$, through which a tensor with the size of $I_1 \times I_2 \times \cdots \times I_N$ is derived. Thus, the system plant in high-order tensor form can be obtained by substituting the gridded varying parameters into the original plant.

3 Problem Formulation

This section discusses the derivation process for the attitude dynamic model, which is based on the hybrid coordinate method [24]. It is assumed that the variation of the attitude angle is relatively small, so the linearization of kinematics equation is employed to simplify the kinetics [25]. Considering a rigid body with two rotational flexible appendages, the system dynamic model can be written as follow [1]:

$$\begin{cases} \mathbf{J}(\delta)\ddot{\theta} + \displaystyle\sum_{i=1}^{2} \boldsymbol{\Delta}_i(\delta)\ddot{\boldsymbol{\eta}}_i = \mathbf{u} + \mathbf{d} \\ \ddot{\boldsymbol{\eta}}_i + 2\boldsymbol{\xi}_i \boldsymbol{\Omega}_i \dot{\boldsymbol{\eta}}_i + \boldsymbol{\Omega}_i^2 \boldsymbol{\eta}_i + \boldsymbol{\Delta}_i^T(\delta)\ddot{\boldsymbol{\theta}} = \mathbf{0} \end{cases} \tag{4}$$

where $i = 1, 2$ are the north/south rotational appendages. δ represents the rotational angle. $\mathbf{J}(\delta)$ represents the inertia matrix varying with δ. $\boldsymbol{\theta}$ denotes the Euler angles of the spacecraft, $\boldsymbol{\Delta}_i(\delta)$, $\boldsymbol{\eta}_i$, $\boldsymbol{\xi}_i$, and $\boldsymbol{\Omega}_i$ represent the coupling coefficient matrices for the appendages vibration and spacecraft rotation, modal coordinates, modal damping ratios and the modal frequencies of the ith appendage, respectively. $\mathbf{u}$ represents the control torque, and $\mathbf{d}$ is the disturbance torque.

If we define vector $\mathbf{x}_p = [\boldsymbol{\theta}^T, \boldsymbol{\eta}_1^T, \boldsymbol{\eta}_2^T]^T, \boldsymbol{\eta}_1 \in R^{n_1 \times 1}$, and $\boldsymbol{\eta}_2 \in R^{n_2 \times 1}$. As in Ref. [25], it is assumed that the attitude angles and attitude velocities can be measured by sensors. Thus, if we denotes $\mathbf{y}_p$ as the measurements, then the state equation of Eq. (4) can be synthetically written by

$$\begin{cases} \dot{\mathbf{x}}_p = \mathbf{A}_p \mathbf{x}_p + \mathbf{B}_p(\mathbf{u} + \mathbf{d}) \\ \mathbf{y}_p = \mathbf{C}_p \mathbf{x}_p \end{cases} \tag{5}$$

where

$$\mathbf{A}_p = \begin{bmatrix} \mathbf{0}_{3+n_1+n_2} & \mathbf{I}_{3+n_1+n_2} \\ -\mathbf{M}(\delta)^{-1}\mathbf{K} & -\mathbf{M}(\delta)^{-1}\mathbf{D} \end{bmatrix}, \quad \mathbf{B}_p = \begin{bmatrix} \mathbf{0}_{(3+n_1+n_2)\times 3} \\ \mathbf{M}(\delta)^{-1}\mathbf{H} \end{bmatrix},$$

$$\mathbf{C}_p = \begin{bmatrix} \mathbf{H}^T & \mathbf{0} \\ \mathbf{0} & \mathbf{H}^T \end{bmatrix}, \quad \mathbf{M}(\delta) = \begin{bmatrix} \mathbf{J}(\delta) & \boldsymbol{\Delta}_1(\delta) & \boldsymbol{\Delta}_2(\delta) \\ \boldsymbol{\Delta}_1^T(\delta) & \mathbf{I}_{n_1} & \mathbf{0}_{n_1 \times n_2} \\ \boldsymbol{\Delta}_2^T(\delta) & \mathbf{0}_{n_2 \times n_1} & \mathbf{I}_{n_2} \end{bmatrix},$$

$$\mathbf{D} = \begin{bmatrix} \mathbf{0}_{3\times 3} & \mathbf{0}_{3\times n_1} & \mathbf{0}_{3\times n_2} \\ \mathbf{0}_{n_1\times 3} & 2\boldsymbol{\xi}_1\boldsymbol{\Omega}_1 & \mathbf{0}_{n_1\times n_2} \\ \mathbf{0}_{n_2\times 3} & \mathbf{0}_{n_2\times n_1} & 2\boldsymbol{\xi}_2\boldsymbol{\Omega}_2 \end{bmatrix},$$

$$\mathbf{K} = \begin{bmatrix} \mathbf{0}_{3\times 3} & \mathbf{0}_{3\times n_1} & \mathbf{0}_{3\times n_2} \\ \mathbf{0}_{n_1\times 3} & \boldsymbol{\Omega}_1^2 & \mathbf{0}_{n_1\times n_2} \\ \mathbf{0}_{n_2\times 3} & \mathbf{0}_{n_2\times n_1} & \boldsymbol{\Omega}_2^2 \end{bmatrix}, \quad \mathbf{H} = \begin{bmatrix} \mathbf{I}_3 \\ \mathbf{0}_{n_1\times 3} \\ \mathbf{0}_{n_2\times 3} \end{bmatrix}$$

$\mathbf{I}_3$ represents a unit matrix with three dimensions. The subsequent discussion is based on Eq. (5). Here, we rewrite the original plant described by Eq. (5) into a system matrix. After applying HOSVD, the obtained high-order tensor can be transformed as follows:

$$\begin{aligned} \mathbf{G}_p(\delta) &= \begin{bmatrix} \mathbf{A}_p & \mathbf{B}_p \\ \mathbf{C}_p & \mathbf{0} \end{bmatrix} = \mathbf{G}_{pn}^E \otimes_{n=1}^N \boldsymbol{\sigma}_n(\delta_n) \\ \mathbf{G}_{pn}^E &:= \begin{bmatrix} \mathbf{A}_{pn}^E & \mathbf{B}_{pn}^E \\ \mathbf{C}_{pn}^E & \mathbf{0} \end{bmatrix} \in R^{I_1 \times I_2 \times \cdots \times I_N \times m \times l} \end{aligned} \tag{6}$$

where $\mathbf{G}_p(\delta)$ is the parameter varying plant with the size of $m \times l$, δ (rotational angle) represents the varying parameter vector, $\mathbf{G}_{pn}^E$ represents the ith subtensor of the core tensor with the size of $I_1 \times I_2 \times \cdots \times I_N \times m \times l$, and $\boldsymbol{\sigma}_n(\delta)$ is the weighting coefficient of each subtensor, which satisfies the properties described in Ref. [23]. With the earlier process, the derived polytopic LPV form reduces the computational complexity when solving the controller synthesis condition. This transformation can be regarded as an approximation to the original plant when some modes with small norms being truncated. The bound of this error is quantified by the quadratic sum of the abandoned modes singular values.

4 Gain Scheduling Controller Synthesis

4.1 Generalized Plant. The main focus of this section is to implement the attitude tracking as well as to guarantee the robustness against disturbances and residual modes. Consider that the controller gain can be calculated in the analogous structure of Eq. (6). Inspired by the weighting function design techniques proposed in Ref. [26], the generalized plant is depicted in Fig. 1.

In Fig. 1, $\mathbf{G}_p(\delta, t)$ is the approximation of the original LPV system based on HOSVD. W_1 is a weighting function accounting for high frequency modes. W_2 is related to the error between reference signals and measured values. $\mathbf{d}$ and $\boldsymbol{\delta}$ are the disturbance torques and varying parameters, respectively. The inputs of the controller are the error between the reference signal $\mathbf{r}$ and the system output in Eq. (5), while its outputs are the torques applied on the body axes of the spacecraft. Figure 1 shows that the controller is self-scheduling via an online tuning unit. Every vertex controller is time invariant, while the coefficient of each one is a function of δ corresponding to the output of the online tuning unit. It is

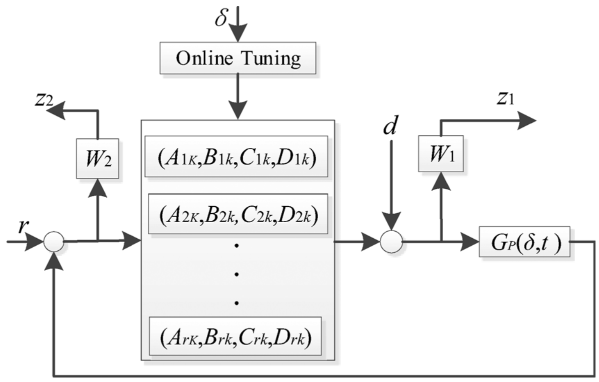

Fig. 1 The generalized plant with online tuning unit

noted that both weighting functions $W_1(s)$ and $W_2(s)$ are assumed to be a sixth-order system with the model structure of

$$\begin{cases} \dot{\mathbf{x}}_i = \mathbf{A}_{ti}\mathbf{x}_i + \mathbf{B}_{ti}\omega_i \\ \mathbf{z}_i = \mathbf{C}_{ti}\mathbf{x}_i \end{cases}, \quad (i = 1, 2) \tag{7}$$

where $(\mathbf{A}_{ti}, \mathbf{B}_{ti}, \mathbf{C}_{ti})$ are the constant system matrices and $\boldsymbol{\omega}_i$ represents the corresponding inputs. With the aforementioned information, if we denote $\mathbf{x} = [\mathbf{x}_p^T, \mathbf{x}_1^T, \mathbf{x}_2^T]^T$ as the system state, the generalized plant can be represented by

$$\begin{cases} \dot{\mathbf{x}} = \mathbf{A}(\delta)\mathbf{x} + \mathbf{B}_1(\delta)\boldsymbol{\omega} + \mathbf{B}_2(\delta)\mathbf{u} \\ \mathbf{z} = \mathbf{C}_1\mathbf{x} \\ \mathbf{y} = \mathbf{C}_2\mathbf{x} + \mathbf{D}_{21}\boldsymbol{\omega} \end{cases} \tag{8}$$

$$\mathbf{A}(\delta) = \begin{bmatrix} \mathbf{A}_p(\delta) & \mathbf{0} & \mathbf{0} \\ \mathbf{0} & \mathbf{A}_{t1} & \mathbf{0} \\ -\mathbf{B}_{t2}\mathbf{C} & \mathbf{0} & \mathbf{A}_{t2} \end{bmatrix}, \quad \mathbf{B}_1(\delta) = \begin{bmatrix} \mathbf{B}_p(\delta) & \mathbf{0} \\ \mathbf{B}_{t1} & \mathbf{0} \\ \mathbf{0} & \mathbf{B}_{t2} \end{bmatrix},$$

$$\mathbf{B}_2(\delta) = \begin{bmatrix} \mathbf{B}_p(\delta) \\ \mathbf{B}_{t1} \\ \mathbf{0} \end{bmatrix}, \quad \mathbf{C}_1 = \begin{bmatrix} \mathbf{0} & \mathbf{C}_{t1} & \mathbf{0} \\ \mathbf{0} & \mathbf{0} & \mathbf{C}_{t2} \end{bmatrix},$$

$$\mathbf{C}_2 = \begin{bmatrix} -\mathbf{C} & \mathbf{0} & \mathbf{0} \end{bmatrix}, \quad \mathbf{D}_{21} = \begin{bmatrix} \mathbf{0} & \mathbf{I} \end{bmatrix}$$

where $\mathbf{z}$ is the controlled output, $\mathbf{y}$ is the measurements, and $\mathbf{u}$ is the control input. It should be noted that the zero in system matrices represents a null matrix with appropriate dimensions. Equation (8) provides the basic LPV model in Sec. 4.2.

4.2 Controller Synthesis. Consider an LPV system in the state-space form as Eq. (8). Replace $(\mathbf{A}_p, \mathbf{B}_p, \mathbf{C}_p, \mathbf{0})$ from Eq. (6) into Eq. (8). When the N in Eq. (6) equals 1, the polytopic plant of the generalized system is derived as follows:

$$\mathbf{G}_g \in \complement \circ \left\{ \begin{bmatrix} \mathbf{A}_i & \mathbf{B}_{1i} & \mathbf{B}_{2i} \\ \mathbf{C}_1 & \mathbf{0} & \mathbf{0} \\ \mathbf{C}_2 & \mathbf{D}_{21} & \mathbf{0} \end{bmatrix}, \quad i = 1, 2, \ldots, \varepsilon \right\} \tag{9}$$

where $\mathbf{A}_i, \mathbf{B}_{1i}, \ldots$, represent the system matrices of each LTI vertex. ε is the number of LTI vertexes. Similarly, with $N = 1$, the controller can be described in the following form:

$$\begin{bmatrix} \mathbf{A}_k(\delta) & \mathbf{B}_k(\delta) \\ \mathbf{C}_k(\delta) & \mathbf{D}_k(\delta) \end{bmatrix} = \sum_{i=1}^{\varepsilon} \sigma_i(\delta(t)) \begin{bmatrix} \mathbf{A}_{ki} & \mathbf{B}_{ki} \\ \mathbf{C}_{ki} & \mathbf{D}_{ki} \end{bmatrix} \tag{10}$$

where $(\mathbf{A}_{ki}, \mathbf{B}_{ki}, \mathbf{C}_{ki}, \mathbf{D}_{ki})$ denotes the ith vertex of the controller. $\sigma_i(\delta)$ is the weighting coefficient, which is a function of δ.

The aim of this section was to derive the controller synthesis condition when the closed-loop LPV system satisfies internal stability and to guarantee the controlled output $\mathbf{z}$ has a L_2-gain bound γ against disturbance $\boldsymbol{\omega}$ [10]. It is assumed that the time-varying parameter and it variation rate are bounded. The given LPV plant is in the form of Eq. (8) with a control value depicted by Eq. (10). By extending the general H_∞ suboptimal control synthesis theorem, this LPV control synthesis problem can be resolved with the following Theorem:

THEOREM 1. *For the system (9) with a feedback controller, the closed-loop LPV system is quadratically stable and the L_2 gain of $||\mathbf{z}(t)||_2/||\boldsymbol{\omega}(t)||_2$ is bounded, if and only if there exists a continuously differentiable matrix function $\mathbf{P}(\delta) = \mathbf{P}^T(\delta) > \mathbf{0}$, a positive scalar γ and continuous matrix functions $(\mathbf{A}_k, \mathbf{B}_k, \mathbf{C}_k, \mathbf{D}_k)$ satisfying the following LMIs:*

$$\begin{bmatrix} \mathbf{P}\mathbf{A}_{cl} + \mathbf{A}_{cl}^T\mathbf{P} + \dot{\mathbf{P}} & \mathbf{P}\mathbf{B}_{cl} & \mathbf{C}_{cl}^T \\ * & -\gamma\mathbf{I} & \mathbf{D}_{cl}^T \\ * & * & -\gamma\mathbf{I} \end{bmatrix} < \mathbf{0} \tag{11}$$

*where $(\mathbf{A}_{cl}, \mathbf{B}_{cl}, \mathbf{C}_{cl}, \mathbf{D}_{cl})$ represent the state-space matrices of the closed-loop system. Every matrix except $\mathbf{I}$ in this theorem varies with δ. The symbol * denotes corresponding symmetrical matrices.*

Proof. Denote a Lyapunov function as $V = \frac{1}{2}\mathbf{x}^T\mathbf{P}(\delta)\mathbf{x}$. From Eq. (11), it can be deduced that $\mathbf{P}\mathbf{A}_{cl} + \mathbf{A}_{cl}^T\mathbf{P} + \dot{\mathbf{P}} < \mathbf{0}$, the closed-loop system is quadratically stable. By applying the Schur complement, Eq. (11) can be rewritten as follows:

$$\begin{bmatrix} \mathbf{C}_{cl}^T \\ \mathbf{D}_{cl}^T \end{bmatrix} [\mathbf{C}_{cl}\mathbf{D}_{cl}] + \begin{bmatrix} \mathbf{A}_{cl}^T\mathbf{P} + \mathbf{P}\mathbf{A}_{cl} + \dot{\mathbf{P}} & \mathbf{P}\mathbf{B}_{cl} \\ \mathbf{B}_{cl}^T\mathbf{P} & -\gamma^2\mathbf{I} \end{bmatrix} < \mathbf{0} \tag{12}$$

By multiplying the left side of the inequality with $[\mathbf{x}^T\boldsymbol{\omega}^T]$ and $[\mathbf{x}^T\boldsymbol{\omega}^T]^T$, it can be transformed into $\mathbf{z}^T\mathbf{z} - \gamma^2\boldsymbol{\omega}^T\boldsymbol{\omega} + \mathbf{x}^T\mathbf{P}\dot{\mathbf{x}} + \frac{1}{2}\mathbf{x}^T\dot{\mathbf{P}}\mathbf{x}$. Integrate the result from 0 to T. Then, Eq. (12) can be transformed as follows:

$$\int_0^T [\mathbf{z}^T\mathbf{z} - \gamma^2\boldsymbol{\omega}^T\boldsymbol{\omega} + \dot{\mathbf{V}}]dt < \mathbf{0} \tag{13}$$

Thus, with the zeros initial assumption, it is obvious that the system output $\mathbf{z}$ and input $\boldsymbol{\omega}$ satisfy $||\mathbf{z}||_2 < \gamma||\boldsymbol{\omega}||_2$.

Remark 2. Generally, a conservative but commonly used technique is to assume $\mathbf{P}(\delta)$ to be a constant matrix. That is to say, every varying parameter value corresponds to the same matrix $\mathbf{P}$. To reduce this conservativeness, $\mathbf{P}$ is defined with a similar structure as matrix $\mathbf{A}(\delta)$. Consequently, when the controller is substituted by a polytopic one with the assumption that $\mathbf{B}_2$, $\mathbf{C}_2$ are simultaneously parameter-independent, then the aforementioned theorem can be rewritten as

THEOREM 2. *For the system (9) with the control law (10), the closed-loop LPV system is quadratically stable and the L_2 gain of $||\mathbf{z}(t)||_2/||\boldsymbol{\omega}(t)||_2$ is bounded, if and only if there exists parameter-dependent symmetric matrix functions $\mathbf{X}(\delta) := \sum \sigma_i(\delta)\mathbf{X}_i > \mathbf{0}$, $\mathbf{Y}(\delta) := \sum \sigma_i(\delta)\mathbf{Y}_i > 0$, parameter-dependent matrices $(\hat{\mathbf{A}}_{ki}, \hat{\mathbf{B}}_{ki}, \hat{\mathbf{C}}_{ki}, \hat{\mathbf{D}}_{ki})$ and a positive scalar γ satisfying the LMIs in Eqs. (14) and (15). Consequently, the synthesis problem can be modified as follows:*

$$\min \gamma$$

$$\text{subject to (14) and (15) hold}, \ \forall(\delta, \dot{\delta}) \in [\underline{\delta}, \bar{\delta}] \times [\underline{\dot{\delta}}, \bar{\dot{\delta}}] \tag{14}$$

$$\begin{bmatrix} \mathbf{X}_i & \mathbf{I} \\ \mathbf{I} & \mathbf{Y}_i \end{bmatrix} > \mathbf{0}, (i, j = 1, \ldots, \varepsilon)$$

$$
\begin{bmatrix}
\mathbf{A}_j\mathbf{X}_i + \mathbf{B}_2\hat{\mathbf{C}}_j + (*)^T & * & * & * \\
\hat{\mathbf{A}}_j + (\mathbf{A}_j + \mathbf{B}_2\hat{\mathbf{D}}_j\mathbf{C}_2)^T & \mathbf{Y}_i\mathbf{A}_j + \hat{\mathbf{B}}_j\mathbf{C}_2 + (*)^T & * & * \\
\mathbf{B}_1^T + (\mathbf{B}_2^T\hat{\mathbf{D}}_j\mathbf{D}_{21})^T & (\mathbf{Y}_i\mathbf{B}_1 + \hat{\mathbf{B}}_j\mathbf{D}_{21})^T & -\gamma\mathbf{I} & * \\
\mathbf{C}_1\mathbf{X}_i + \mathbf{D}_{12}\hat{\mathbf{C}}_j & \mathbf{C}_1 + \mathbf{D}_{12}\hat{\mathbf{D}}_j\mathbf{C}_2 & \mathbf{D}_{11} + \mathbf{D}_{12}\hat{\mathbf{D}}_j\mathbf{D}_{21} & -\gamma\mathbf{I}
\end{bmatrix} < \mathbf{0} \tag{15}
$$

Proof. Due that $\mathbf{G}(\delta)$ is defined of polytopic structure, the system state-space matrix can be depicted as $\mathbf{G} := \sum_{i=1}^{\varepsilon} \sigma_i(\delta(t))\mathbf{G}_i$. It is noted that σ_i represents the weighting coefficients varying with $\delta(t)$ satisfying $\sum_{i=1}^{\varepsilon} \sigma_i(\delta) = 1$. By substituting the polytopic LPV state-space matrices into Eq. (11), there exists the following equation:

$$
\begin{bmatrix}
\sum_{i=1}^{\varepsilon}\sigma_i^2\mathbf{P}_i\mathbf{A}_{cli} + \sum_{i,j=1,i\neq j}^{\varepsilon}\sigma_i\sigma_j\mathbf{P}_i\mathbf{A}_{clj} + (*) + \dot{\mathbf{P}} & \sum_{i=1}^{\varepsilon}\sigma_i^2\mathbf{P}_i\mathbf{B}_{cli} + \sum_{i,j=1,i\neq j}^{\varepsilon}\sigma_i\sigma_j\mathbf{P}_i\mathbf{B}_{clj} & \mathbf{C}_{cl}^T \\
* & -\gamma\mathbf{I} & \mathbf{D}_{cl}^T \\
* & * & -\gamma\mathbf{I}
\end{bmatrix} < \mathbf{0} \tag{16}
$$

Consider $1 = (\sum_{i=1}^{\varepsilon}\sigma_i)(\sum_{i=1}^{\varepsilon}\sigma_i)$. Equation (16) is rewritten as the following equation:

$$
\sum_{i=1}^{\varepsilon}\sigma_i^2
\begin{bmatrix}
\mathbf{P}_i\mathbf{A}_{cli} + (*) + \dot{\mathbf{P}} & \mathbf{P}_i\mathbf{B}_{cli} & \mathbf{C}_{cl}^T \\
* & -\gamma\mathbf{I} & \mathbf{D}_{cl}^T \\
* & * & -\gamma\mathbf{I}
\end{bmatrix}
+ \sum_{i,j=1,i\neq j}^{\varepsilon}\sigma_i\sigma_j
\begin{bmatrix}
\mathbf{P}_i\mathbf{A}_{clj} + (*) + \dot{\mathbf{P}} & \mathbf{P}_i\mathbf{B}_{clj} & \mathbf{C}_{cl}^T \\
* & -\gamma\mathbf{I} & \mathbf{D}_{cl}^T \\
* & * & -\gamma\mathbf{I}
\end{bmatrix} < \mathbf{0} \tag{17}
$$

Thus, if the following condition exists at every vertex, Eq. (17) is satisfied simultaneously:

$$
\begin{bmatrix}
\mathbf{P}_i\mathbf{A}_{clj} + (*) + \dot{\mathbf{P}} & \mathbf{P}_i\mathbf{B}_{clj} & \mathbf{C}_{cl}^T \\
* & -\gamma\mathbf{I} & \mathbf{D}_{cl}^T \\
* & * & -\gamma\mathbf{I}
\end{bmatrix} < \mathbf{0}, (i, j = 1, 2, \ldots, \varepsilon) \tag{18}
$$

Partition $\mathbf{P}_i$ and $\mathbf{P}_i^{-1}$ as follows:

$$
\mathbf{P}_i = \begin{bmatrix} \mathbf{Y}_i & \mathbf{N}_i \\ \mathbf{N}_i^T & \mathbf{S} \end{bmatrix}, \quad \mathbf{P}_i^{-1} = \begin{bmatrix} \mathbf{X}_i & \mathbf{V}_i \\ \mathbf{V}_i^T & \mathbf{Z}_i \end{bmatrix}
$$

where $\mathbf{X}_i$, $\mathbf{Y}_i$ are symmetrical matrices and $\mathbf{N}_i$, $\mathbf{V}_i$ are in fit dimension. Denote that

$$
\mathbf{\Gamma}_{1i} = \begin{bmatrix} \mathbf{X}_i & \mathbf{I} \\ \mathbf{V}_i^T & \mathbf{0} \end{bmatrix}, \quad \mathbf{\Gamma}_{2i} = \begin{bmatrix} \mathbf{I} & \mathbf{Y}_i \\ \mathbf{0} & \mathbf{N}_i^T \end{bmatrix}
$$

There exits $\mathbf{P}_i\mathbf{\Gamma}_{1i} = \mathbf{\Gamma}_{2i}$. Pre- and postmultiply Eq. (18) by $\text{diag}\{\mathbf{\Gamma}_i^T, \mathbf{I}, \mathbf{I}\}$ and $\text{diag}\{\mathbf{\Gamma}_i, \mathbf{I}, \mathbf{I}\}$, respectively. If $(\hat{\mathbf{A}}_{kj}, \hat{\mathbf{B}}_{kj}, \hat{\mathbf{C}}_{kj}, \hat{\mathbf{D}}_{kj})$ are derived as in Ref. [10], then Eq. (15) can be deduced easily. With the constraint of Eq. (14), $\mathbf{P}_i > 0$ is guaranteed.

Remark 3. Although this theorem requires a parameter-independent $\mathbf{B}_2$, which is different from the derived LPV system in Eq. (8), it can be realized by adding postfiltering with the control inputs $\mathbf{u}$ [27]. The mathematic model of this filter is given by

$$
\begin{cases}
\dot{\mathbf{x}}_f = \mathbf{A}_f\mathbf{x}_f + \mathbf{B}_f\mathbf{u} \\
\mathbf{u}_f = \mathbf{A}_f\mathbf{x}_f
\end{cases} \tag{19}
$$

where $\mathbf{A}_f$ is stable, $\mathbf{u}$ is the input, and $\mathbf{u}_f$ is the output. With this modification, the original dependence on δ in the control input matrix is eliminated. The original plant is depicted in Fig. 2.

5 Numerical Example

This section presents numerical simulations on a flexible spacecraft attitude control problem. The overall inertia can be calculated with the following equation as in Ref. [28]:

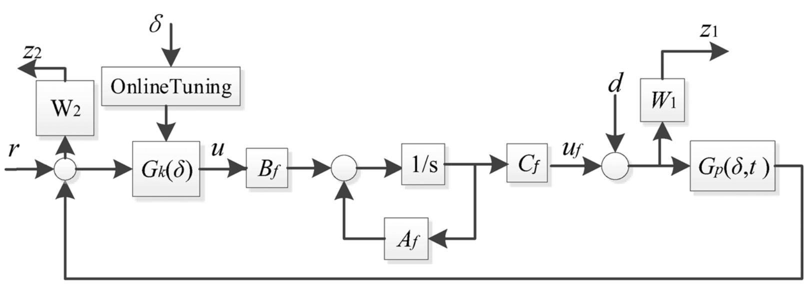

Fig. 2 The modified generalized plant with online tuning unit

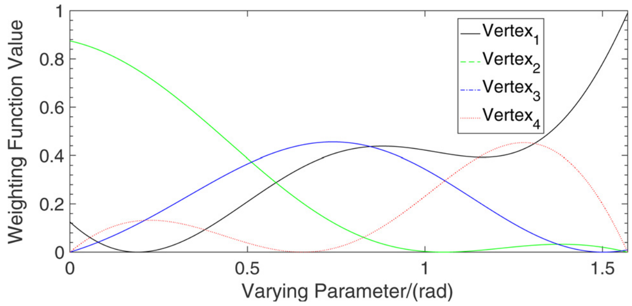

Fig. 3 Weighting function value changing with varying parameters

$$\mathbf{J}(\delta) = \mathbf{J}_b + \sum_{i=1}^{2} \mathbf{J}_{ai}\mathbf{C}_i(\delta) - \sum_{i=1}^{2} m_{ai}\mathbf{r}_{ai}^{\times}\mathbf{r}_{ai}^{\times}, \ (i = 1, 2)$$

where $\mathbf{J}_b$, $\mathbf{J}_{ai}$, and m_{ai} are the rigid body inertia, rotating appendages inertia, and the mass of appendages, respectively. $\mathbf{C}_i(\delta)$ and $\mathbf{J}_{ai}$ are the appendages coordinate transformation matrices and cross product matrices of the corresponding installation position, respectively. The varying parameter is defined in $\Omega = [0\,\text{deg}, 90\,\text{deg}]$, which is divided into 150 discretized grids. It is noted that the varying parameter is in periodic variations, and the condition when rotation angle in other intervals resembles that of Ω. Thus, it is reasonable to restrict the parameter domain. Conditions in other intervals can be easily derived. After implement-

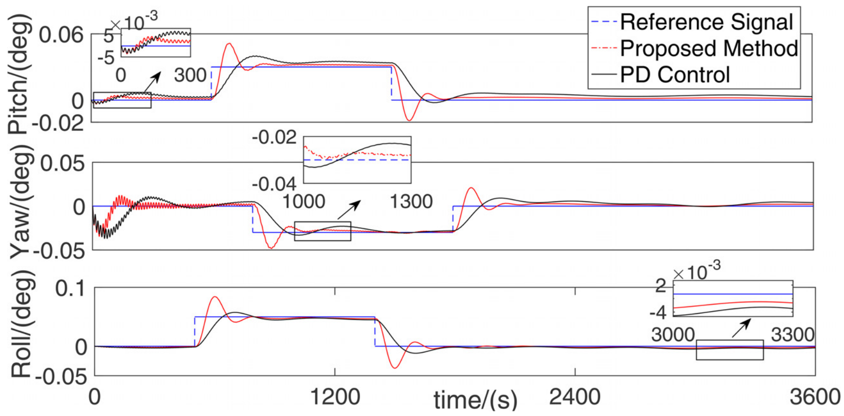

Fig. 4 Roll, pitch, and yaw angles when tracking reference signal

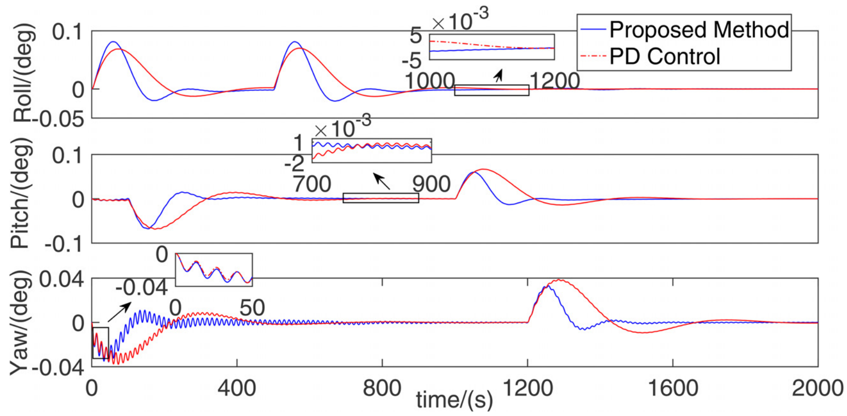

Fig. 5 Roll, pitch, and yaw angles when disturbed by square wave torques

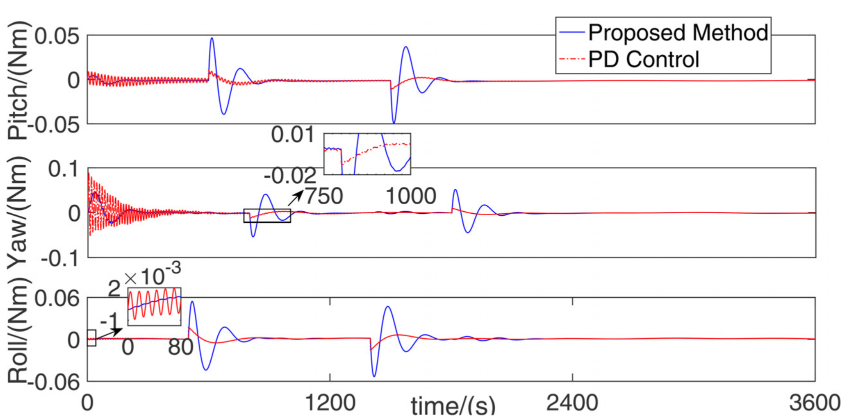

Fig. 6 Roll, pitch, and yaw control inputs for signal tracking

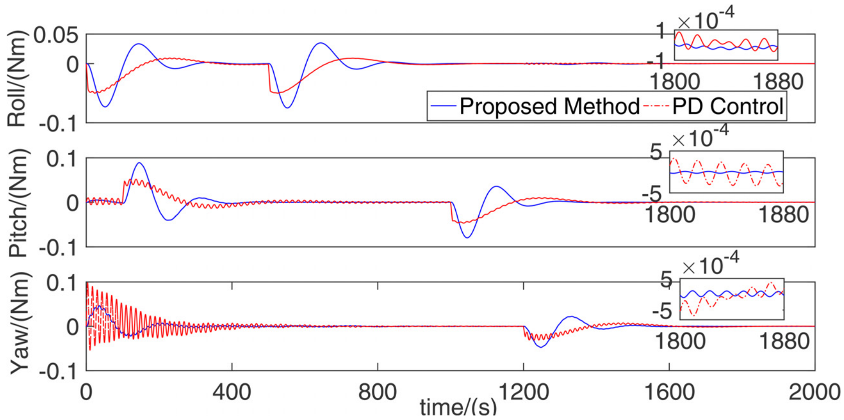

Fig. 7 Roll, pitch, and yaw control inputs when disturbed by square wave torques

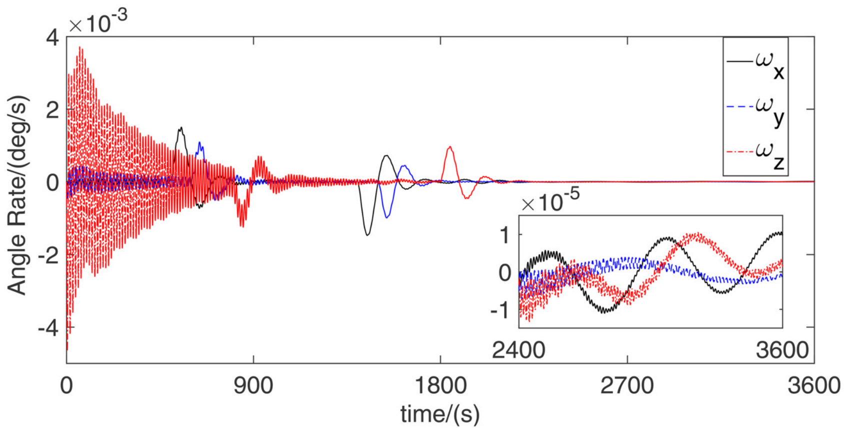

Fig. 8 Roll, pitch, and yaw angular rates in proposed methods when tracking reference signal

ing HOSVD, the original LPV system can be converted into the polytopic form as Eq. (9). The variation regulation of the weighting coefficients is shown in Fig. 3.

From Fig. 3, it is noted that the vertex number is 4, which is the result of ε in Eq. (9). The value of the weighting function denotes the proportion of every LTI system at certain varying parameter values. These weighting values are used in the convex combination of vertex controllers when applying control missions. When receiving the input parameter, the online tuning part outputs the real-time weighting coefficients by interpolating the obtained coefficient group.

By solving the controller synthesis condition in Eqs. (14) and (15), each vertex controller gain can be obtained. To verify performances of the proposed control scheme, the simulations are carried out under the following cases:

Case 1. Reference tracking control, in which the reference attitude angle commands are set, as shown in Fig. 4 with solid lines.

Case 2. Square wave interference, in which the disturbances are set as 0.5 N·m, 0.5 N·m, and 0.3 N·m corresponding to roll, pitch, and yaw axes.

It is noted that both solar panel rotations and the environmental disturbances are considered in the earlier conditions. The space environmental disturbance torque **d** is set as

$$\mathbf{d} = 0.001 \times \begin{cases} 0.3\cos(10\omega_0 t) + 0.4\sin(3\omega_0 t) - 1 \\ 0.3\cos(5\omega_0 t) - 0.2\sin(2\omega_0 t) + 1.5 \\ 0.3\sin(10\omega_0 t) - 0.8\sin(4\omega_0 t) + 1 \end{cases}$$

The initial Euler angles and the angle rates are set at $[0, 0, 0, 0, 0, 0]^T$. In addition, the initial first-order modal coordinate and its time derivative are set at 0.1 and 0.01, respectively.

In the first case, Fig. 4 shows the time response of pitch, roll, and yaw attitude angles tracking reference commands. Compared with the given proportional-derivative (PD) control result, the proposed method provides faster convergence and higher stabilization precision. By calculating the root-mean-square of the results after 3550 s, the attitude control accuracy and stability of the proposed method are 3×10^{-5} deg and 2×10^{-7} deg/s, compared with the 9×10^{-5} deg and 3×10^{-7} deg/s using PD control.

In the second case, according to Fig. 5, it is clear that the gain-scheduling LPV control resists the square wave interference with less fluctuation and faster stabilization. In this case, the proposed method is 2×10^{-6} deg in attitude control accuracy and 6×10^{-7} deg/s in stability, while the conventional PD control is 9×10^{-6} deg in attitude control accuracy and 1×10^{-7} deg/s in stability.

As illustrated in both Figs. 6 and 7, the proposed control technique reduces chattering in the output torques with a reasonable amplitude, although it entails larger control torques than the conventional PD control. From Figs. 8 and 9, it is obvious that the proposed method can suppress modal vibration.

6 Conclusions

This paper proposes a self-scheduling controller to solve the attitude control problem for large flexible satellites with rotational appendages. It is found that the introduction of HOSVD technique successfully provides a model transformation process to derive a

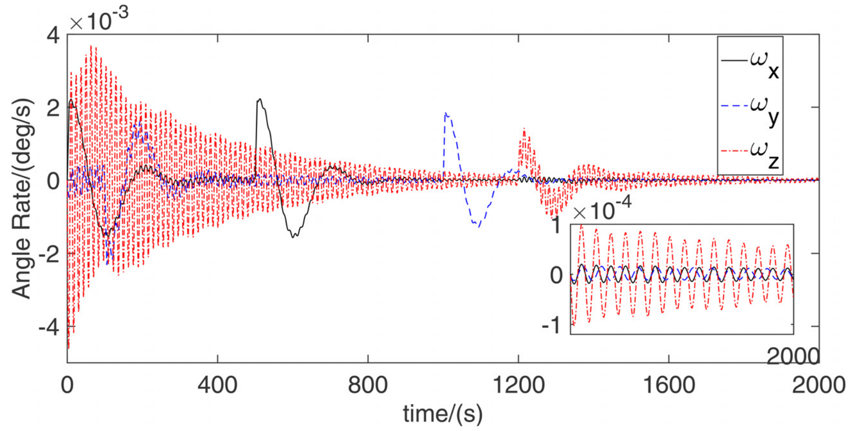

Fig. 9 Roll, pitch, and yaw angular rates in proposed methods when disturbed by square wave torques

polytopic LPV model with varying weighting values. The control performances can be realized by adding corresponding weighting functions into a generalized plant. With the introduction of LPV H_∞ control theory, the controller synthesis problem is transformed into a convex optimization problem with a family of LMIs to solve. Analysis shows that the controller conservativeness is reduced by using a parameter-dependent Lyapunov function, instead of a single constant one.

Numerical results demonstrate that the proposed controller outperforms a conventional PD controller, with better settling time and precision. Moreover, the proposed control method exhibits less computational complexity in comparison with conventional methods of controlling a flexible satellite. Further research is required to examine the measurement error and optimize the controller gain in future.

Funding Data

- Chinese Academy of Sciences (LSU-2016-07-02).
- National Natural Science Foundation of China (11572019).

References

[1] Nagashio, T., Kida, T., Ohtani, T., and Hamada, Y., 2010, "Design and Implementation of Robust Symmetric Attitude Controller for ETS-VIII Spacecraft," Control Eng. Pract., **18**(12), pp. 1440–1451.

[2] Guy, N., Alazard, D., Cumer, C., and Charbonnel, C., 2014, "Dynamic Modeling and Analysis of Spacecraft With Variable Tilt of Flexible Appendages," ASME J. Dyn. Syst. Meas. Control, **136**(2), p. 021020.

[3] Bahrami, M., and Kalantari Nezhad, R., 2006, "Adaptive Attitude Control of a Flexible Satellite," First International Symposium on Systems and Control in Aerospace and Astronautics, Harbin, China, Jan. 19–21, pp. 1329–1333.

[4] Gransden, D. I., and Mooij, E., 2016, "Simple Adaptive Control of a Satellite With Large Flexible Appendages," 67th International Astronautical Congress, Guadalajara, Mexico, Sept. 26–30, p. 13.

[5] Hu, Q., 2009, "Robust Adaptive Sliding Mode Attitude Maneuvering and Vibration Damping of Three-Axis-Stabilized Flexible Spacecraft With Actuator Saturation Limits," Nonlinear Dyn., **55**(4), pp. 301–321.

[6] Xiao, B., Yin, S., and Gao, H., 2018, "Reconfigurable Tolerant Control of Uncertain Mechanical Systems With Actuator Faults: A Sliding Mode Observer-Based Approach," IEEE Trans. Control Syst. Technol., **26**(4), pp. 1249–1258.

[7] Xiao, B., Dong, Q., Ye, D., Liu, L., and Huo, X., 2018, "A General Tracking Control Framework for Uncertain Systems With Exponential Convergence Performance," IEEE/ASME Trans. Mechatronics, **23**(1), pp. 111–120.

[8] Xiao, B., Yin, S., and Kaynak, O., 2016, "Tracking Control of Robotic Manipulators With Uncertain Kinematics and Dynamics," IEEE Trans. Ind. Inf., **63**(10), pp. 6439–6449.

[9] Rugh, W. J., and Shamma, J. S., 2000, "Research on Gain Scheduling," Automatica, **36**(10), pp. 1401–1425.

[10] Apkarian, P., and Adams, R. J., 1998, "Advanced Gain-Scheduling Techniques for Uncertain Systems," IEEE Trans. Control Syst. Technol., **6**(1), pp. 21–32.

[11] Lu, B., and Wu, F., 2004, "Switching LPV Control Designs Using Multiple Parameter-Dependent Lyapunov Functions," Automatica, **40**(11), pp. 1973–1980.

[12] Chen, P. C., Wu, S. L., and Chuang, H. S., 2010, "The Smooth Switching Control for TORA System Via LMIs," Eighth IEEE International Conference on Control and Automation, Xiamen, China, June 9–11, pp. 1338–1343.

[13] Hanifzadegan, M., and Nagamune, R., 2014, "Smooth Switching LPV Controller Design for LPV Systems," Automatica, **50**(5), pp. 1481–1488.

[14] Jiang, W., Dong, C., and Wang, Q., 2015, "Smooth Switching Linear Parameter-Varying Control for Hypersonic Vehicles Via a Parameter Set Automatic Partition Method," IET Control Theory Appl., **9**(16), pp. 2377–2386.

[15] Shamma, J. S., and Cloutier, J. R., 1993, "Gain-Scheduled Missile Autopilot Design Using Linear Parameter Varying Transformations," J. Guid. Control Dyn., **16**(2), pp. 256–263.

[16] Cai, G., Song, J., and Chen, X., 2014, "Robust LPV Autopilot Design for Hypersonic Reentry Vehicle," Aircr. Eng. Aerosp. Technol., **86**(5), pp. 423–431.

[17] Shen, Y., Yu, J., Luo, G., and Mei, Y., 2017, "Missile Autopilot Design Based on Robust LPV Control," J. Syst. Eng. Electron., **28**(3), pp. 536–545.

[18] Leici, F. D. B. C., and Leici, R. J. M. C., 2007, *Wind Turbine Control Systems*, Springer Verlag, London.

[19] Shirazi, F. A., Grigoriadis, K. M., and Viassolo, D., 2012, "Wind Turbine Integrated Structural and LPV Control Design for Improved Closed-Loop Performance," Int. J. Control, **85**(8), pp. 1178–1196.

[20] Bagherieh, O., and Nagamune, R., 2015, "Gain-Scheduling Control of a Floating Offshore Wind Turbine Above Rated Wind Speed," Control Theory Technol., **13**(2), pp. 160–172.

[21] Szeidl, L., Baranyi, P., Petres, Z., and Varlaki, P., 2007, "Numerical Reconstruction of the HOSVD Based Canonical Form of Polytopic Dynamic Models," Third International Symposium on Computational Intelligence and Intelligent Informatics, Agadir, Morocco, Mar. 28–30, pp. 111–116.

[22] Jiang, W., Wang, H., Lu, J., and Xie, Z., 2016, "HOSVD-Based LPV Modeling and Mixed Robust H_2/H_∞ Control Design for Air-Breathing Hypersonic Vehicle," Syst. Eng. Electron., **27**(1), pp. 183–191.

[23] Petres, Z., 2006, "Polytopic Decomposition of Linear Parameter-Varying Models by Tensor-Product Model Transformation," Ph.D. thesis, Budapest University of Technology and Economics, Budapest, Hungary.

[24] Likins, P. W., 1970, "Dynamics and Control of Flexible Space Vehicles," National Aeronautics and Space Administration, Pasadena, CA, JPL Technical Report No. NASA-CR-105592, JPL-TR-32-1329.

[25] Hamada, Y., Ohtani, T., Kida, T., and Nagashio, T., 2006, "A New Gain Scheduling Controller Synthesis and Its Application to Attitude Control Systems of a Large Flexible Satellite," IEEE International Conference on Control Applications, Munich, Germany, Oct. 4–6, pp. 2914–2920.

[26] Hanifzadegan, M., and Nagamune, R., 2015, "Tracking and Structural Vibration Control of Flexible Ballscrew Drives With Dynamic Variations," IEEE/ASME Trans. Mechatronics, **20**(1), pp. 133–142.

[27] Kwon, S., Shimomura, T., and Okubo, H., 2011, "Pointing Control of Spacecraft Using Two SGCMGs Via LPV Control Theory," Acta Astronaut., **68**(7–8), pp. 1168–1175.

[28] Nagashio, T., Kida, T., Hamada, Y., and Ohtani, T., 2014, "Robust Two-Degrees-of-Freedom Attitude Controller Design and Flight Test Result for Engineering Test Satellite-VIII Spacecraft," IEEE Trans. Control Syst. Technol., **22**(1), pp. 157–168.